HEAVY FERMIONS

# Shot noise in a strange metal

Liyang Chen[1], Dale T. Lowder[2], Emine Bakali[3], Aaron Maxwell Andrews[4], Werner Schrenk[5], Monika Waas[3], Robert Svagera[3], Gaku Eguchi[3], Lukas Prochaska[3], Yiming Wang[2], Chandan Setty[2], Shouvik Sur[2], Qimiao Si[2], Silke Paschen[3], Douglas Natelson[2,6,7]*

S trange-metal behavior has been observed in materials ranging from high-temperature superconductors to heavy fermion metals. In conventional metals, current is carried by quasiparticles; although it has been suggested that quasiparticles are absent in strange metals, direct experimental evidence is lacking. We measured shot noise to probe the granularity of the current-carrying excitations in nanowires of the heavy fermion strange metal $YbRh_2Si_2$. When compared with conventional metals, shot noise in these nanowires is strongly suppressed. This suppression cannot be attributed to either electron-phonon or electron-electron interactions in a Fermi liquid, which suggests that the current is not carried by well-defined quasiparticles in the strange-metal regime that we probed. Our work sets the stage for similar studies of other strange metals.

Strange metals are non-Fermi liquids that exhibit a low temperature ($T$) electrical resistivity contribution that is directly proportional to $T$ (*1*). This response has been reported across many materials families, including cuprate (*2*–*4*) and pnictide (*5*) superconductors, ruthenates (*6*), heavy fermion metals (*7*–*9*), and twisted bilayer graphene (*10*). Strange-metal properties typically arise at finite temperature above a quantum critical point (QCP), often in proximity to antiferromagnetic order (*11*). There are two broad classes of theories on metallic QCPs. Within the standard Landau approach of order parameter fluctuations, quasiparticles retain their integrity (*12*, *13*). By contrast, in approaches beyond the Landau framework (*14*–*18*), no long-lived quasiparticles are expected to remain. Thus, determining the nature of the low-energy current-carrying excitations is an important means to elucidate the nature of strange metals near QCPs.

How can we determine whether the current carriers in strange metals are quasiparticles? Shot noise in electrical conduction (*19*) is a distinctive probe of mesoscopic systems in which the current noise, $S_I = \langle (I - \langle I \rangle)^2 \rangle$, in a system driven out of equilibrium accesses the nature of the charge-carrying excitations. Here, $I$ is the instantaneous current and $\langle I \rangle$ is the average current. The Fano factor, $F$, gives the ratio between the measured noise $S_I$ and $2e\langle I \rangle$, the expectation for Poissonian transport of ordinary "granular" charge carriers of magnitude $e$ with an average current $\langle I \rangle$. Shot noise has revealed fractionalization of charge in the fractional quantum Hall liquid (*20*, *21*), fractional effective charges in quantum dot Kondo systems (*22*, *23*), and pairing in superconducting nanostructures in the normal state (*24*, *25*). A lack of granular quasiparticles would naïvely be expected to suppress shot noise, because the flow of a continuous fluid should have no fluctuations.

Despite their ubiquity, strange metals have yet to be examined through shot-noise measurements for several technical reasons, and only a few relevant theoretical predictions exist for any quantum critical systems (*26*, *27*). In many materials, strange metallicity is cut off at low temperatures by the onset of superconductivity, which complicates matters because shot-noise measurements also require an electrical bias $eV$, where $e$ is the charge of the electron and $V$ is the applied voltage, that is large compared with the thermal scale $k_BT$ to distinguish from thermal noise, where $k_B$ is the Boltzmann constant. Tunneling transport into a strange metal faces the challenge that only discrete, individual electrons can be added or removed, which likely leads to noise dominated by single-electron effects. Fortunately shot noise can be measured within a material using a diffusive mesoscopic wire, which requires the nanofabrication of such structures without affecting electronic properties—a major challenge for many materials.

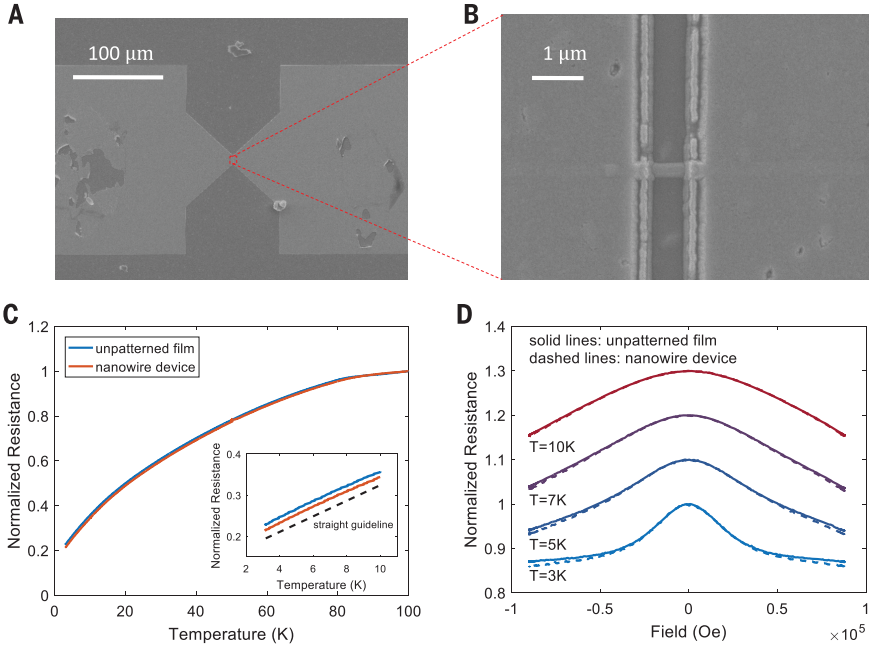


**Fig. 1. $YbRh_2Si_2$ nanowire device preparation and characterization.** (**A**) $YbRh_2Si_2$ nanowire between two large-area, thick-sputtered Au contacts on top of the unpatterned $YbRh_2Si_2$ film, which were deposited to ensure that the measured voltage is dominated by the nanowire. (**B**) Higher-magnification view of the indicated region in (A). Sample fabrication is discussed in detail in (*33*). (**C**) Normalized resistance as a function of temperature for both the unpatterned film and the etched nanowire. The inset shows that resistivity in the low-temperature limit in both the film and the wire is linear in temperature (with black dashed line as a linear-in-temperature guide to the eye), as seen previously (*31*). Unpatterned film resistance at 100 K is 17.8 ohms. Nanowire resistance at 100 K is 164.7 ohms. (**D**) Normalized resistance as a function of the in-plane magnetic field for both the unpatterned molecular-beam epitaxy film and the etched nanowire (magnetic field $B$ is oriented transverse to the nanowire), with curves shifted vertically for clarity. Zero-field resistances for the film at 10, 7, 5, and 3 K (top to bottom) are 6.5, 5.5, 4.8, and 4.1 ohms, respectively. Zero-field resistances for the wire at 10, 7, 5, and 3 K are 57.8, 49.0, 42.2, and 35.5 ohms, respectively. The nearly identical response between the nanowire and the unpatterned film confirms that patterning did not substantially alter the electronic properties of the epitaxial $YbRh_2Si_2$ material and that the resistance is dominated by the wire.

[1]Applied Physics Graduate Program, Rice University, TX 77005, USA. [2]Department of Physics and Astronomy, Rice Center for Quantum Materials, Rice University, Houston, TX 77005, USA. [3]Institute of Solid State Physics, TU Wien, Wiedner Hauptstraße 8-10, 1040 Vienna, Austria. [4]Institute of Solid State Electronics, TU Wien, Gußhausstraße 25-25a, Gebäude CH, 1040 Vienna, Austria. [5]Center for Micro and Nanostructures, TU Wien, Gußhausstraße 25-25a, Gebäude CH, 1040 Vienna, Austria. [6]Department of Electrical and Computer Engineering, Rice University, Houston, TX 77005, USA. [7]Department of Materials Science and NanoEngineering, Rice University, Houston, TX 77005, USA.
*Corresponding author. Email: natelson@rice.edu

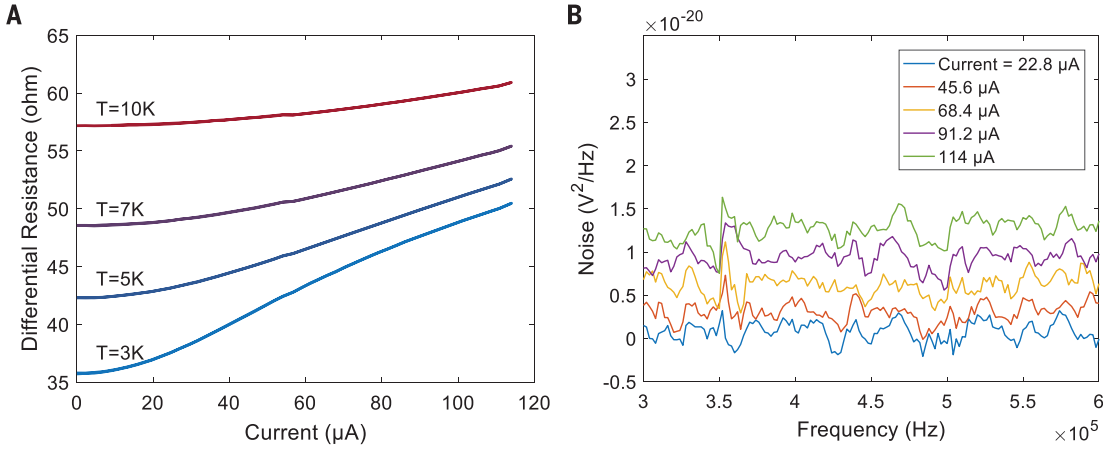


**Fig. 2. Noise characterization of a $YbRh_2Si_2$ nanowire.** (**A**) Differential resistance d*V*/d*I* as a function of bias current at 10, 7, 5, and 3 K (top to bottom). Comparison with theoretical shot-noise expectations requires this information (see Eqs. 1 and 2). (**B**) Averaged voltage noise spectra (with zero-bias spectra subtracted) of a $YbRh_2Si_2$ nanowire device at different bias levels at $T$ = 3 K, over a bandwidth between 300 and 600 kHz. This spectral range is free of extrinsic features, and these voltage noise spectra are analyzed (Eq. 2) to determine the shot noise at each bias. Each spectrum shown is an average of 4500 spectra with 10-kHz bandwidth.

We have successfully made mesoscopic wires for noise measurements from epitaxial films of the heavy fermion material $YbRh_2Si_2$, a particularly well-defined strange metal (*9*, *28*). $YbRh_2Si_2$ has a zero-temperature magnetic field–induced continuous quantum phase transition from a low-field antiferromagnetic heavy Fermi liquid metal to a paramagnetic one. The Hall effect displays a rapid isothermal crossover that extrapolates to a jump at the QCP in the zero-temperature limit, which provides evidence for a sudden reconstruction of the Fermi surface across the QCP and an associated change in the nature of the quasiparticles between the two phases (*29*), as expected in the Kondo destruction description (*14*–*16*) for a beyond-Landau QCP. At finite temperatures, a quantum critical fan of strange metallicity extends over a broad range of temperature and magnetic field (*28*, *30*). Recent time-domain THz transmission measurements (*31*) of the optical conductivity of epitaxial films of $YbRh_2Si_2$ reveal the presence of quantum critical charge fluctuations below 15 K, supporting the Kondo destruction picture in this system.

Measuring shot noise in $YbRh_2Si_2$ wires directly examines how current flows in a system thought to lack discrete charge excitations; these results can then be compared with predictions in Fermi liquids. We report measurements of shot noise in mesoscopic wires patterned from epitaxial films of $YbRh_2Si_2$, examined below 10 K, in the strange-metal regime where phonon scattering is not expected to be relevant to the conductivity. The measured shot noise is found to be far smaller than both weak- and strong electron-electron scattering expectations for Fermi liquids and also smaller than the values measured on a gold nanowire for comparison. Furthermore, the electron-phonon coupling that was determined experimentally using long $YbRh_2Si_2$ nanowires rules out strong electron-phonon scattering as a noise-suppression mechanism. Therefore, the suppressed shot noise is evidence that current-carrying excitations in this strange metal defy a quasiparticle description in the examined temperature range. The no-quasiparticle model described in previous work (*26*, *27*), despite being derived using conformal field theory for different kinds of QCP and associated phases than those of $YbRh_2Si_2$, predicts nontrivial bias- and temperature-dependent noise that is qualitatively consistent with the observed trends.

### Measuring shot noise in $YbRh_2Si_2$ devices

High-quality epitaxial films of $YbRh_2Si_2$ were grown by molecular beam epitaxy on germanium substrates (*31*, *32*) [see section 3 in (*33*) for details]. The temperature dependence of the resistivity of these films above 3 K shows strange-metal properties ($\rho = \rho_0 + AT^{\alpha}$, where $\alpha \approx 1$ in the low temperature limit, $\rho$ is is the electrical resistivity, and $A$ is the temperature coefficient) as in the bulk material (Fig. 1C).

The films are patterned into nanowires through a combination of electron-beam lithography and reactive ion etching (see fig. S2 and the accompanying discussion). The nanowire shown in Fig. 1B is 60 nm thick, 660 nm long, and 240 nm in width. Thick source and drain contact pads ensure that the dominant voltage measured under bias is across the nanowire; the contact pads also act as thermal sinks (*34*). An important concern in fabricating nanostructures from strongly correlated materials is that the patterning process does not alter the underlying physics. As shown in Fig. 1C, the resistance $R(T)$ of the nanowire closely matches that of the unpatterned film, including a dominant linear-in-$T$ dependence at low temperatures. Similarly, in Fig. 1D, the magnetoresistance (field in-plane, perpendicular to the current) in the nanowire is nearly identical to that of the unpatterned film, showing that the fabrication process did not alter the material's properties. This consistency also shows that the total $R$ is dominated by the wire, because the large contacts are coated in thick gold and would not exhibit such a magnetoresistance. Three nanowires patterned from this same film all show essentially identical transport and noise properties (data from devices 2 and 3 are shown in fig. S5).

The noise-measurement technique is well developed (*21*, *24*, *34*). A current bias is applied to the device by means of a heavily filtered voltage source and ballast resistors. Using a custom probe, the voltage across the device is measured through two parallel sets of amplifiers and a high-speed data acquisition system (fig. S1C). The time-series data are cross-correlated and Fourier transformed to yield the voltage noise $S_V$ across the device, with the correlation mitigating the amplifier input noise [see sections 1 and 2 of (*33*) for a detailed discussion of calibration and averaging]. Figure 2A shows the variation of the differential resistance, d*V*/d*I*, as a function of bias current, whereas Fig. 2B gives examples of voltage noise spectra at several bias currents at a base temperature of 3 K. At the maximum bias currents that were applied, the voltage drop across the wire is several mV, a bias energy scale that considerably exceeds $k_BT$ (0.25 meV at 3 K), as is needed for shot noise measurements.

### Theoretical expectations for the shot noise and Fano factor

To understand the measured noise in $YbRh_2Si_2$, we first considered the expected current shot noise result for a diffusive metallic constriction. This is a long-established calculation within the Landauer-Büttiker formalism (*35*–*39*) for a Fermi gas (i.e., without any electron-electron interactions). A metal with well-defined quasiparticles is assumed in the source and drain, which obey the Fermi-Dirac (FD) distribution with a temperature set by the contacts, $T_0$. In the noninteracting, nanoscale limit, conduction takes place through spin-degenerate quantum channels with various transmittances, $\tau_i$. Each channel contributes to $S_I$ by an amount proportional to $\tau_i(1 - \tau_i)$. By averaging over the distribution of transmittances (*35*–*38*), one finds a predicted Fano factor

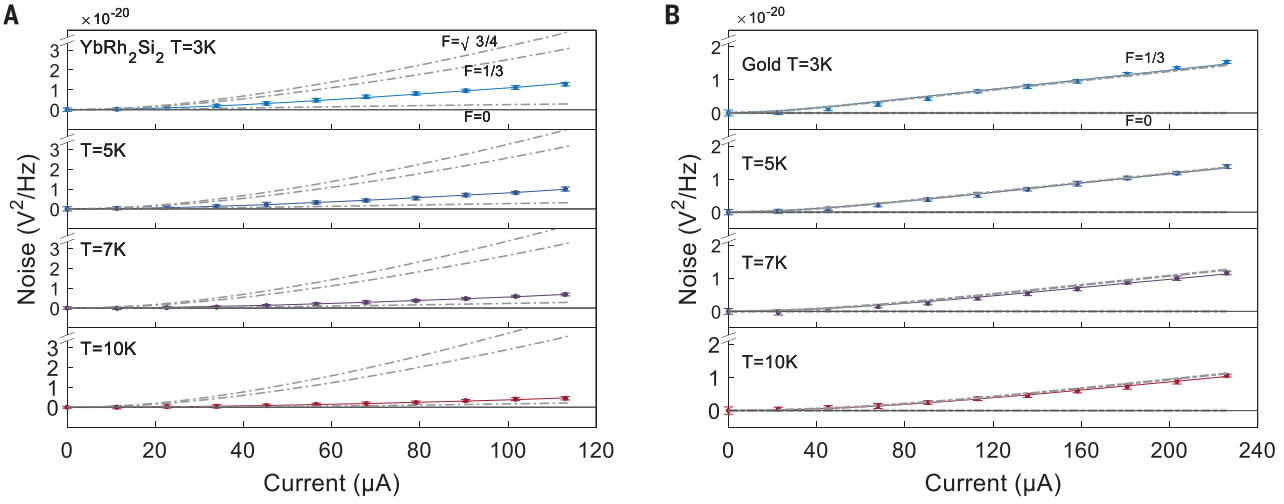


**Fig. 3. Noise versus bias current characteristics.** (**A**) Noise versus bias current for a $YbRh_2Si_2$ wire at 10, 7, 5, and 3 K (top to bottom), with fits to Eq. 1 to extract effective Fano factors. Error bars are the standard deviation from 15 repeated bias-sweep measurements. Also shown for illustrative purposes are expectations for $F = \sqrt{3}/4, 1/3$ and 0 (indicated by the gray dot-dashed curves from top to bottom, respectively), which were calculated by using the measured differential resistance at each temperature and Eq. 2. At all temperatures, the measured voltage noise is far below the theoretical expectations for shot noise in a diffusive nanowire of a Fermi liquid, even in the weak electron-electron scattering limit. (**B**) Analogous data for a gold wire over the same temperature range, as discussed in section 9 of (*33*). Data here are much closer to the $F = 1/3$ Fermi liquid expectation, with the small deviation at the highest temperatures being attributed to electron-phonon scattering effects. Error bars are the standard deviation from 15 repeated bias-sweep measurements.

$F \equiv S_I/2e\langle I\rangle = 1/3$. When inelastic electron-electron scattering is added to the otherwise noninteracting Fermi system, such that the system size along the direction of the current exceeds the electron-electron scattering length, $L > L_{ee}$ (see fig. S11) but is smaller than the electron-phonon scattering length, $L_{ph}$, there is a redistribution of energy and effective thermalization among the carriers (*40*, *41*). There is a local quasi-thermal FD distribution within the wire described by a local electronic temperature $T_e(x)$ that is higher than the lattice temperature, $T_0 = T$, which is assumed to be uniform and equal to the temperature of the contacts. This approach leads to a prediction of $F = \sqrt{3}/4 \approx 0.433$ (*40*, *41*). Fano factor predictions in both $L < L_{ee} < L_{ph}$ and $L_{ph} > L > L_{ee}$ limits have been confirmed in experiments in mesoscopic metal wires (*34*, *42*–*44*).

In the present context, an important question is what happens in a Fermi liquid state when the electron-electron interactions are so strong that the quasiparticle weight is orders of magnitude smaller than the noninteracting case (equal to 1) for a free electron (though still nonzero) and the Landau parameters are correspondingly large. It was recently shown that charge conservation constrains the Fano factor to be independent of the quasiparticle weight, and the combination of instantaneous electronic interactions and Poissonian charge transport dictates that the shot noise and average current get renormalized identically by the Landau parameters (*45*). As a result, for this regime (see solid line in fig. S11) that pertains to a strongly correlated Fermi liquid of interest here, the Fano factor would be $F = \sqrt{3}/4 \approx 0.433$. [For further details, see section 13 of (*33*) and (*45*).]

Within the Fermi liquid quasiparticle picture, the only way to suppress shot noise below these levels is through strong electron-phonon scattering, which perturbs the electronic distribution function. In the limit of very strong electron-phonon coupling, the electronic distribution is constrained to be in equilibrium with the lattice temperature, $T_0$, and only Johnson-Nyquist noise at $T_0$ remains.

### Comparison to theoretical expectations

Figure 3 shows the measured voltage noise as a function of bias current for a $YbRh_2Si_2$ nanowire, and its counterpart for a gold nanowire for comparison. Shown as gray dot-dashed lines are the $F = 1/3$ expectations based on the measured differential resistance, $dV/dI$. Independent of any detailed analysis, the measured noise in the $YbRh_2Si_2$ wire is clearly suppressed well below the Fermi liquid expectation at all temperatures. Additional data on two more wires (devices 2 and 3) are essentially identical [see section 7 of (*33*) and fig. S5]. By contrast, the gold nanowire data [discussed further in section 9 of (*33*) and fig. S7] are consistent with Fermi liquid predictions, with a slight suppression of the noise above 10 K as electron-phonon scattering becomes relevant (fig. S7D).

The electron-phonon coupling may be extracted experimentally by analyzing the noise as a function of bias in a wire sufficiently long that electron-phonon scattering is dominant (*42*). As detailed in section 5 of (*33*), we performed this analysis using a 30-μm-long $YbRh_2Si_2$ wire to determine the effective electron-phonon coupling in this material and found a value sufficiently small that strong electron-phonon scattering is ruled out as a mechanism for suppressing the noise in the much shorter $YbRh_2Si_2$ nanowire constrictions.

Extracting effective Fano factors from the measured noise requires analysis in terms of finite temperature expressions for the shot noise. Subtleties about thermal noise can arise when the device is non-ohmic, as discussed in section 10 of (*33*), but corrections from the ohmic case are small for the measured nonlinearities shown in Fig. 2A. The expected form for the current shot noise in an ohmic system with Fano factor $F$ and differential resistance $dV/dI$ is (*19*)

$$S_I = F \cdot 2e\langle I\rangle \coth\left(\frac{eV}{2k_BT}\right) + (1-F)4k_BT\left(\frac{dV}{dI}\right)^{-1} \quad (1)$$

This expression reduces to the Johnson-Nyquist current noise $S_{I,JN} = 4k_BT\left(\frac{dV}{dI}\right)^{-1}_{I=0}$ in the zero-bias limit and becomes $S_I = F \cdot 2e\langle I\rangle$ as expected in the high-bias limit $eV \gg k_BT$. In the experiment, we measured voltage noise, and, for ease of comparison, we subtracted off the zero-bias Johnson-Nyquist noise so that effective Fano factors may be estimated by fitting to the voltage-based expression for the shot noise:

$$S_V = \left(\frac{dV}{dI}\right)^2_I \left[F \cdot 2e\langle I\rangle \coth\left(\frac{eV}{2k_BT}\right) + (1-F)4k_BT\left(\frac{dV}{dI}\right)^{-1}_1\right] - 4k_BT\left(\frac{dV}{dI}\right)_{I=0} \quad (2)$$

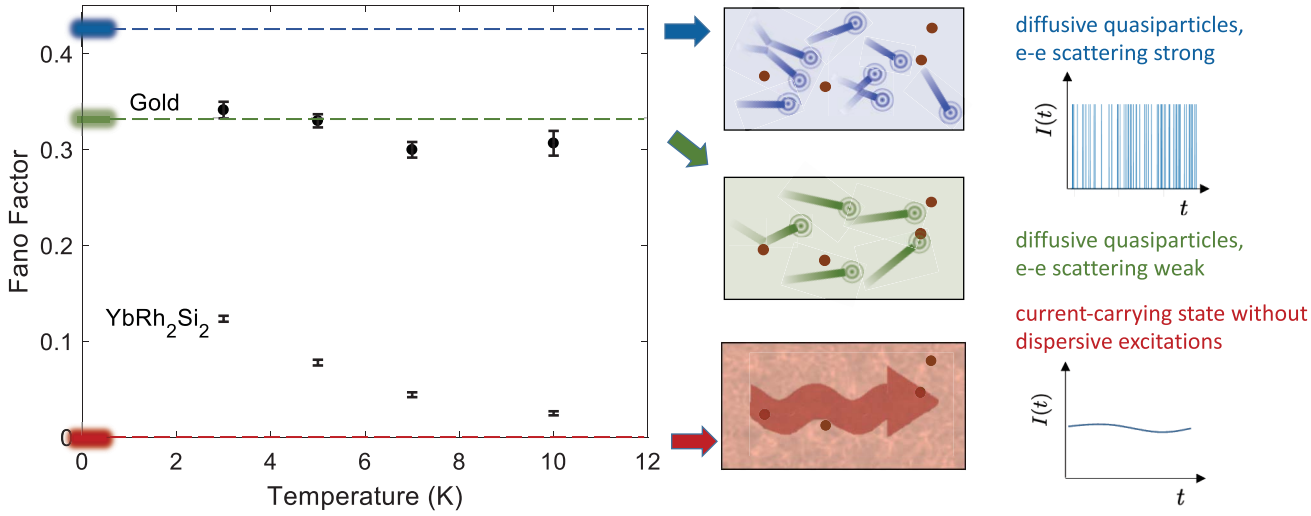


**Fig. 4. Fano factors and context for their interpretation.** Fano factors found from fitting the data in Fig. 3 are shown. Error bars are the standard error from fitting 15 repeated bias sweep measurements. In a Fermi liquid, current is carried by individual quasiparticle excitations, and the current as a function of time fluctuates with the arrival of each discrete transmitted carrier. Carriers scatter diffusively through static disorder (brown dots). When electron-electron scattering is weak (sample length $L < L_{ee}$), the expected Fano factor is $F = 1/3$ (green mark in the graph), whereas electron-phonon coupling can suppress this at higher temperatures. When electron-electron scattering is strong ($L > L_{ee}$), the expected Fano factor is $F = \sqrt{3}/4$ (blue mark in the graph). In a system without well-defined quasiparticles, charge transport is more continuous, which leads to suppressed current fluctuations; in the extreme limit, where electronic excitations are entirely nondispersive, the Fano factor is expected to vanish (red mark). Dashed lines are guides to the eye.

The fitted Fano factors of a $YbRh_2Si_2$ device and a gold nanowire device are shown in Fig. 4, which provides a direct comparison between $YbRh_2Si_2$ and a Fermi liquid diffusive wire. Corrections stemming from the nonohmic response lead to lower inferred Fano factors (fig. S8).

Our detailed thermal modeling of the present system under the standard Fermi liquid assumptions [see section 6 of (*33*)] confirms that, including electronic thermal transport through the Wiedemann-Franz relation and the measured electron-phonon coupling, $F = \sqrt{3}/4$ would be expected in the present high-bias limit. This is in sharp contrast to the experimental data shown in Fig. 3A. Experiments on bulk $YbRh_2Si_2$ crystals do not show large deviations from the Wiedemann-Franz relation in this temperature range (*46*, *47*). Electronic transport measurements and thermodynamic measurements of $YbRh_2Si_2$ in this temperature regime, as well as THz optical conductivity measurements (*31*) in these films, show that phonons are not contributing strongly to the electronic properties in $YbRh_2Si_2$ below 15 K. As shown in section 6 of (*33*) and fig. S4, the measured electron-phonon coupling in $YbRh_2Si_2$ is too small by more than a factor of 35 to be responsible for the observed noise suppression.

To interpret these results, it is important to consider the nature of quasiparticles in terms of the single-particle spectral function and distribution functions. For a Fermi gas, the single-particle spectral function $A(k, \epsilon)$ at a given wavevector $k$ is a delta function in energy $\epsilon$ at $\epsilon = E_k$, where $E_k$ is the quasiparticle energy as a function of $k$, meaning that a particle excitation at $(k, E_k)$ in the zero temperature limit is perfectly well defined in energy and has an infinite lifetime with a spectral weight $Z = 1$. Correspondingly, the particle excitations follow the FD distribution, and the Fermi surface is a perfectly sharp boundary at $T = 0$. In a Fermi liquid, the spectral function retains a peak for $k$ near the Fermi surface, which describes a quasiparticle with a nonzero spectral weight $Z < 1$. The distribution function near the Fermi surface is smeared but still has a nonzero discontinuity at $T = 0$ K (*48*).

In the case of the particular type of non-Fermi liquid with a complete destruction of quasiparticles, one has $Z = 0$ everywhere on the Fermi surface. With such a complete smearing of the Fermi surface, there is no discontinuity in the distribution function even at $T = 0$ K. In this limit, when driven by a bias that does not greatly perturb the non-FD distribution function, there are no granular quasiparticles that carry the electrical current. We can then expect a much-reduced shot noise, as we observe in the form of a Fano factor that is considerably smaller than not only the strong electron-electron scattering expectation $F = \sqrt{3}/4$ but even the weak electron-electron scattering counterpart $F = 1/3$. We highlight this contrast in Fig. 4 and discuss it further in section 13 of (*33*). For reference, in the extreme case when the electron spectral function at any given $k$ as a function of energy is entirely featureless, the continuous electron fluid would have no shot noise at all ($F = 0$). Interestingly, one approach to a quantum critical system with no quasiparticles (*26*, *27*) predicts nonzero noise with a trend in bias and temperature that is quantitatively similar to that shown in Fig. 3A (as seen in fig. S10), though that model is based on a different form of quantum criticality (a superconductor-insulator transition) than that in $YbRh_2Si_2$. This is discussed further in section 12 of (*33*).

## Discussion and outlook

Shot noise is a probe that gives special access to the nature of charge carriers. The suppressed noise shown in Fig. 3A and summarized in Fig. 4 is evidence that current in this strange-metal regime is not governed by the transport of individual, granular quasiparticles. A Fano factor of zero is expected only for the most extreme case of a non-Fermi liquid that has a completely flat spectral function. A non-Fermi liquid that still has residual dispersive spectral features, despite a vanishing quasiparticle weight $Z$, would lead to a nonzero Fano factor. Any residual dispersive spectral features are naturally expected to somewhat sharpen as $T \to 0$ K, leading to a rise in $F$ as temperature is lowered, but, in that case, would never reach the $F = \sqrt{3}/4$ expectation for a strongly correlated Fermi liquid (where $Z$ is finite). The present experiment takes place firmly in the non-Fermi liquid regime (down to nearly a factor of 10 below the effective single-ion Kondo temperature) that is already seen to exhibit critical scaling of the optical conductivity (*31*). As discussed further in section 13 of (*33*), an effective Fermi liquid

finite temperature correction to the expected Fano factor is not a naturally self-consistent explanation for the trend in Fig. 4. Even so, the present data are limited to 3 K and above; it is desirable to extend our measurements to below 3 K, which would allow for a direct comparison with the $T = 0$ K theoretical expectations.

Although scattering techniques show the incoherent, nonquasiparticle electronic response as a diffuse continuum across ($k$, $\epsilon$), shot noise specifically targets the current-carrying excitations. The shot noise probes both the equilibrium non-Fermi liquid distribution function and its nonequilibrium evolution when perturbed by the difference in source and drain chemical potentials. In Fermi liquids, this approach has provided insights into inelastic electron-electron scattering and the evolution of the nonequilibrium distribution function. This technique will provide crucial experimental constraints on such processes in materials in the strange-metal regime. Moreover, strange metallicity as inferred from the resistivity is observed across many systems with quite disparate underlying microscopic physics (*2*–*8*, *10*, *28*). Shot noise provides an opportunity to test the extent to which these phenomenologically similar strange metals can fit within a single paradigm. We expect our work to trigger extensive further theoretical studies.

## REFERENCES AND NOTES


1. C. M. Varma, *Rev. Mod. Phys.* **92**, 031001 (2020).
2. A. Legros *et al*., *Nat. Phys.* **15**, 142–147 (2019).
3. R. L. Greene, P. R. Mandal, N. R. Poniatowski, T. Sarkar, *Annu. Rev. Condens. Matter Phys.* **11**, 213–229 (2020).
4. J. Ayres *et al*., *Nature* **595**, 661–666 (2021).
5. I. M. Hayes *et al*., *Nat. Phys.* **12**, 916–919 (2016).
6. J. A. N. Bruin, H. Sakai, R. S. Perry, A. P. Mackenzie, *Science* **339**, 804–807 (2013).
7. Hv. Löhneysen *et al*., *Phys. Rev. Lett.* **72**, 3262–3265 (1994).
8. T. Park *et al*., *Nature* **440**, 65–68 (2006).
9. D. H. Nguyen *et al*., *Nat. Commun.* **12**, 4341 (2021).
10. Y. Cao *et al*., *Phys. Rev. Lett.* **124**, 076801 (2020).
11. P. Coleman, A. J. Schofield, *Nature* **433**, 226–229 (2005).
12. J. A. Hertz, *Phys. Rev. B* **14**, 1165–1184 (1976).
13. A. J. Millis, *Phys. Rev. B* **48**, 7183–7196 (1993).
14. Q. Si, S. Rabello, K. Ingersent, J. L. Smith, *Nature* **413**, 804–808 (2001).
15. P. Coleman, C. Pépin, Q. Si, R. Ramazashvili, *J. Phys. Condens. Matter* **13**, R723–R738 (2001).
16. T. Senthil, M. Vojta, S. Sachdev, *Phys. Rev. B* **69**, 035111 (2004).
17. R. A. Davison, K. Schalm, J. Zaanen, *Phys. Rev. B* **89**, 245116 (2014).
18. S. A. Hartnoll, A. Lucas, S. Sachdev, *Holographic Quantum Matter* (MIT Press, 2018).
19. K. Kobayashi, M. Hashisaka, *J. Phys. Soc. Jpn.* **90**, 102001 (2021).
20. R. de-Picciotto *et al*., *Nature* **389**, 162–164 (1997).
21. L. Saminadayar, D. C. Glattli, Y. Jin, B. Etienne, *Phys. Rev. Lett.* **79**, 2526–2529 (1997).
22. T. Delattre *et al*., *Nat. Phys.* **5**, 208–212 (2009).
23. O. Zarchin, M. Zaffalon, M. Heiblum, D. Mahalu, V. Umansky, *Phys. Rev. B* **77**, 241303 (2008).
24. P. Zhou *et al*., *Nature* **572**, 493–496 (2019).
25. K. M. Bastiaans *et al*., *Science* **374**, 608–611 (2021).
26. A. G. Green, J. E. Moore, S. L. Sondhi, A. Vishwanath, *Phys. Rev. Lett.* **97**, 227003 (2006).
27. J. Sonner, A. G. Green, *Phys. Rev. Lett.* **109**, 091601 (2012).
28. J. Custers *et al*., *Nature* **424**, 524–527 (2003).
29. S. Paschen *et al*., *Nature* **432**, 881–885 (2004).
30. P. Gegenwart *et al*., *Phys. Rev. Lett.* **89**, 056402 (2002).
31. L. Prochaska *et al*., *Science* **367**, 285–288 (2020).
32. E. Bakali *et al*., *J. Cryst. Growth* **595**, 126804 (2022).
33. Materials and methods are available as supplementary materials.
34. M. Henny, S. Oberholzer, C. Strunk, C. Schönenberger, *Phys. Rev. B* **59**, 2871–2880 (1999).
35. C. W. J. Beenakker, M. Büttiker, *Phys. Rev. B* **46**, 1889–1892 (1992).
36. K. E. Nagaev, *Phys. Lett. A* **169**, 103–107 (1992).
37. B. L. Altshuler, L. S. Levitov, A. Y. Yakovets, *JETP Lett.* **59**, 857–863 (1994).
38. Y. V. Nazarov, *Phys. Rev. Lett.* **73**, 134–137 (1994).
39. D. B. Gutman, Y. Gefen, *Phys. Rev. B* **64**, 205317 (2001).
40. V. I. Kozub, A. M. Rudin, *Phys. Rev. B* **52**, 7853–7856 (1995).
41. K. E. Nagaev, *Phys. Rev. B* **52**, 4740–4743 (1995).
42. M. Henny *et al*., *Appl. Phys. Lett.* **71**, 773–775 (1997).
43. F. Liefrink, J. I. Dijkhuis, M. J. M. de Jong, L. W. Molenkamp, H. van Houten, *Phys. Rev. B* **49**, 14066–14069 (1994).
44. A. H. Steinbach, J. M. Martinis, M. H. Devoret, *Phys. Rev. Lett.* **76**, 3806–3809 (1996).
45. Y. Wang *et al*., Shot noise as a characterization of strongly correlated metals. arxiv:2211.11735 [cond-mat.str-el] (2022).
46. H. Pfau *et al*., *Nature* **484**, 493–497 (2012).
47. M. Taupin *et al*., *Phys. Rev. Lett.* **115**, 046402 (2015).
48. D. Pines, P. Nozieres, *The Theory of Quantum Liquids Volume I: Normal Fermi Liquids* (Basic Books, 1989).
49. L. Chen *et al*., Data and code for: Shot noise in a strange metal. Zenodo (2023); https://doi.org/10.5281/7800018.


## ACKNOWLEDGMENTS

We acknowledge helpful conversations with M. Foster and A. Lucas. **Funding:** This work was funded by US Department of Energy, Basic Energy Sciences, Experimental Condensed Matter Physics award DE-FG02-06ER46337 (D.N., L.C., D.T.L.); NSF award DMR-1704264 (D.N.); European Research Council ERC Advanced Grant 101055088 (G.E., S.P.); Austrian Science Fund FWF I4047 (E.B., S.P.); Austrian Research Promotion Agency FFG 2156529 (S.P.); Austrian Science Fund FWF SFB F 86 (G.E., S.P.); European Union Horizon 2020 grant agreement 824109-EMP (E.B., G.E., L.P., M.W., R.S., S.P.); Austrian Research Promotion Agency FFG 883941 (W.S., A.M.A.); US Air Force Office of Scientific Research FA8665-22-1-7170 (W.S., A.M.A.); NSF award DMR-2220603 (Y.W., C.S., S.S., Q.S.); Robert A. Welch Foundation Grant C-1411 (Y.W., C.S., S.S., Q.S.); and Vannevar Bush Faculty Fellowship ONR-VB N00014-23-1-2870 (Q.S.). Some of the noise measurement hardware was acquired through NSF award DMR-1704264. **Author contributions:** Growth and characterization of the $YbRh_2Si_2$ films: E.B., W.S., M.W., R.S., G.E., L.P., A.M.A., S.P.; Patterning, device fabrication, noise measurements: L.C., D.T.L.; Noise data analysis and interpretation: L.C., D.N., Q.S., S.P.; Theoretical analysis of Fermi liquid effects: Y.W., C.S., S.S., Q.S.; Critical insights on heavy fermion strange metals: Q.S., S.P.; Writing – initial draft: L.C., D.N., Q.S., S.P.; Writing – editing: L.C., D.T.L., E.B., W.S., M.W., R.S., G.E., L.P., A.M.A., Y.W., C.S., S.S., Q.S., S.P. **Competing interests:** The authors declare no competing financial interests. **Data and materials availability:** All data presented in this paper and the supplementary materials and the relevant analysis code are available through Zenodo (*49*). 

## SUPPLEMENTARY MATERIALS

science.org/doi/10.1126/science.abq6100
Materials and Methods
Supplementary Text
Figs. S1 to S11
References (*50*–*52*)

Submitted 19 April 2022; resubmitted 5 December 2022
Accepted 12 October 2023
10.1126/science.abq6100